

# Fine and Coarse Mode Aerosols in Southern Great Plains Multi-Filter Rotating Shadowband Radiometer Datasets

*M. Alexandrov and B. Cairns  
Columbia University  
New York, New York*

*M. Alexandrov, B E. Carlson, A.A. Lacis, and B. Cairns  
National Aeronautics and Space Administration Goddard Institute for Space Studies  
New York, New York*

## Introduction

We present results obtained using the new version of the multi-filter rotating shadowband radiometer (MFRSR) data analysis algorithm (Alexandrov et al. 2005). This algorithm allows the partition of aerosol optical thickness (AOT) into fine and coarse aerosol modes and to retrieve the fine mode effective radius ( $r_{\text{eff}}$ ). A bimodal gamma distribution is used as the aerosol particle size model. The algorithm has been used for analysis of a multi-year dataset from the local MFRSR network at the U.S. Department of Energy's (DOE's) Atmospheric Radiation Measurement Climate Research Facility (ACRF) Southern Great Plains (SGP) site. The retrieved aerosol parameters are compared with the corresponding AERONET almucantar retrieval results derived from a CIMEL sunphotometer collocated with the MFRSR at the SGP Central Facility. A constrained variant of the algorithm (zero NO<sub>2</sub> column values) has been used to define the range of physically justified values of the fine mode effective radius, and for comparison with AERONET particle size retrievals.

## Geographical Variability of Aerosol Types Across the SGP Site

The time series of the daily mean fine mode aerosol effective radius retrievals for the year 2000 from the Central Facility (E13) and three extended facilities (E2, E4, and E24) are shown in Figure 1. These particular sites were chosen to represent three different aerosol size variability patterns characteristic of these different areas of the SGP site. We identify these types of variability as A, B, and C. As is shown in Figure 2, type A is characteristic to the northeast (e.g., E2) and the southwest of the site, it corresponds to larger 0.3-0.5  $\mu\text{m}$  particles. Type C dominating the southeast (e.g., E24), corresponds to very small aerosol particles with  $r_{\text{eff}}$  less or equal to our detection limit 0.2  $\mu\text{m}$ . Type B intermediate between A and B is encountered in the northwest (e.g., E4) and the central (e.g., E13, which also may be classified as C type) parts of the SGP site. Small and larger particles are present, in this aerosol mass while the latter exhibit seasonality with maximum size in winter. The values of  $r_{\text{eff}}$  obtained using the constrained variant of our algorithm with NO<sub>2</sub> amount set to zero are smaller for type A and B sites compared to type C sites. This may be a result of neglecting of relatively large NO<sub>2</sub> amounts that may actually be present and coming from the same pollution sources as the aerosols. We suggest that the

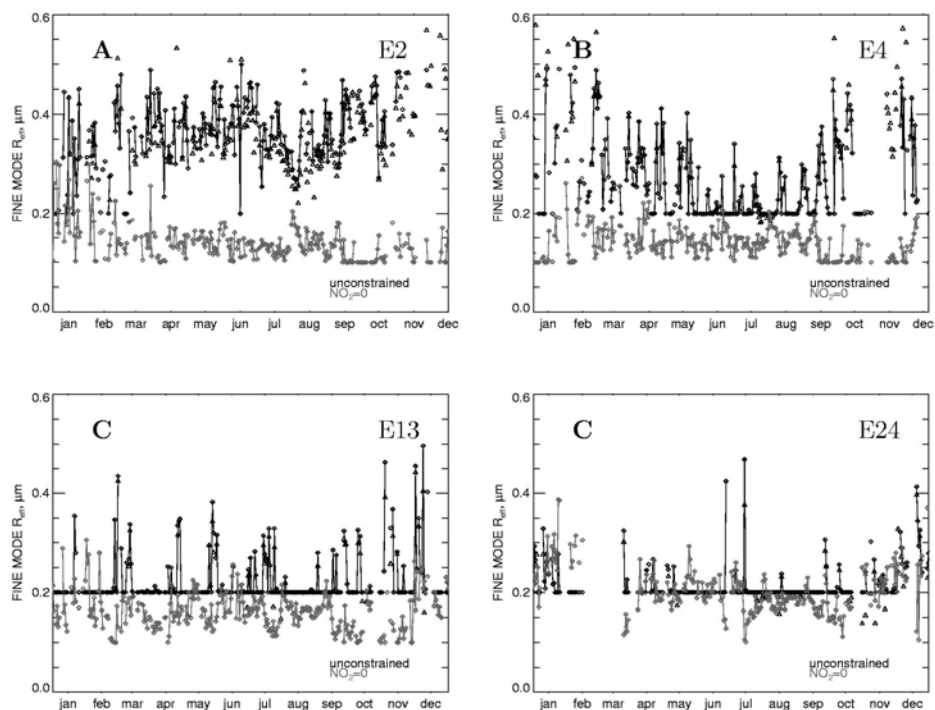


**Figure 1.** Time series of daily mean fine mode effective particle radius for SGP extended facilities E2, E4, E13, and E24 for the year 2000. These illustrate the three characteristic types of variability: **A.** Northeast and southwest of the site, large 0.3 - 0.4  $\mu\text{m}$ ; **B.** Northwest and center, intermediate type with larger particles in winter; **C.** center and southeast, mostly very small fine mode particles (smaller than or equal to the retrieval threshold of 0.2  $\mu\text{m}$ ). E13 can be attributed to both types B and C. Black curves represent values obtained without any constraints on  $\text{NO}_2$  column amounts. Diamonds correspond to retrieved effective radii of bimodal distribution, triangles represent the cases when mode separation was not possible and show  $r_{\text{eff}}$  of the monomodal distributions used. Grey curves show the retrievals with zero  $\text{NO}_2$  condition imposed. They provide the lower bound for possible values of fine  $r_{\text{eff}}$ . The plots reveal larger difference between the constrained and unconstrained retrievals for E2 and E4 located in northern Kansas close to large pollution sources compared to relatively clean E13 and especially E24 sites.

above types of aerosol size variability may reflect a balance between different aerosol species at the SGP site, in particular, sulfates and nitrates. Numerous aerosol sampling studies measuring size distributions of nitrate and sulfate particles confirm, that compared to sulfates, nitrate aerosols have a notably larger concentration of particles with radii exceeding 0.6  $\mu\text{m}$  in their cumulative size distributions. To analyze the relationship between aerosol size and composition we considered sampling measurements performed directly at the SGP's Central Facility by the National Oceanic and Atmospheric Administration's (NOAA's) Pacific Marine Environmental Laboratory (PMEL, <http://saga.pmel.noaa.gov>). These measurements show seasonal cycles in submicron aerosol concentrations with a maximum in winter for nitrates, and in summer for sulfates. The resulting seasonal trend in  $\text{NO}_3/\text{SO}_4$  ratios (Figure 3, left) has a certain resemblance to that in our retrievals of fine mode  $r_{\text{eff}}$  for SGP's Central Facility (E13, Figure 1). It appears that this resemblance goes beyond just seasonal means, but is often present in day-to-day

changes in the concentration ratio as reflected in the corresponding changes in the retrieved effective radius. We illustrate this in a “butterfly” plot (Figure 3, right) comparing the two quantities for days when both are available. In this plot we set the  $\text{NO}_3/\text{SO}_4$  ratios less than 0.05 to zero to reflect the absence of variability in our  $r_{\text{eff}}$  values below the retrieval limit of  $0.2 \mu\text{m}$ . To investigate a possible relationship between geographical differences in retrieved aerosol fine mode effective radius and the spatial variations in aerosol composition, we used the  $\text{NO}_3/\text{SO}_4$  ion concentration ratios obtained from National Atmospheric Deposition Program/National Trends Network (NADP/NTN, <http://nadp.sws.uiuc.edu>) precipitation monitoring sites in Oklahoma, Kansas, and neighboring states. The result of interpolation between the mean values for the year 2000 is shown as a contour plot in Figure 2. This plot shows a trend corresponding to domination of nitrates in A-zones (especially in the north) opposed to domination of sulfates in the C-zone in the southeast of the site. Environmental Protection Administration (EPA) AirData reports (<http://www.epa.gov/air/data/>) indicate that among power plants in the area surrounding the SGP site these located in northeastern Kansas (i.e., in the area where we retrieve larger aerosol sizes) have the largest ratio of  $\text{NO}_x$  to  $\text{SO}_2$  emissions.

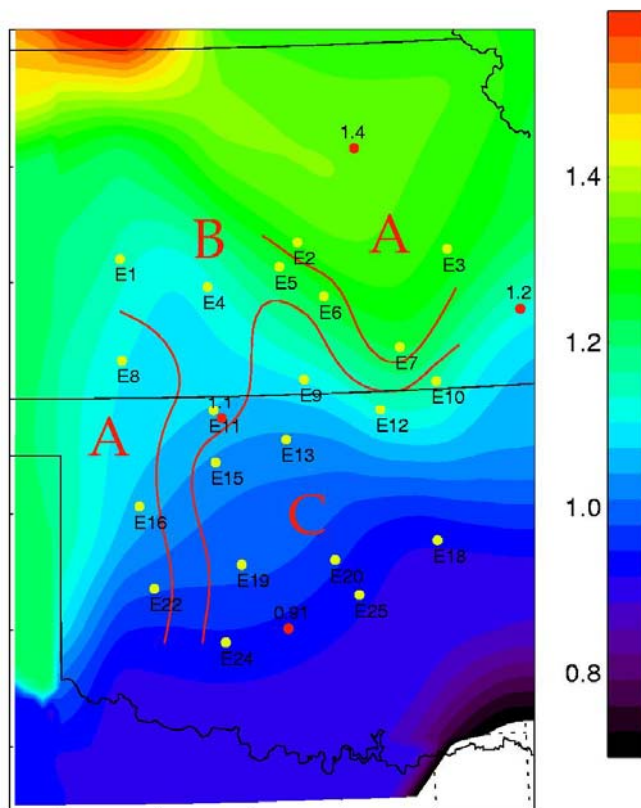


**Figure 2.** Contour plot of the  $\text{NO}_3/\text{SO}_4$  ion concentration ratios (mean values for the year 2000) obtained from National Atmospheric Deposition Program/National Trends Network (NADP/NTN) precipitation monitoring sites (some of them are shown by open circles). The types A and B of aerosol fine particles (see Figure 4) appear to correspond to nitrate-dominated areas, while the smaller particles (type C) are encountered in the sulfate-dominated southeast of the SGP site.

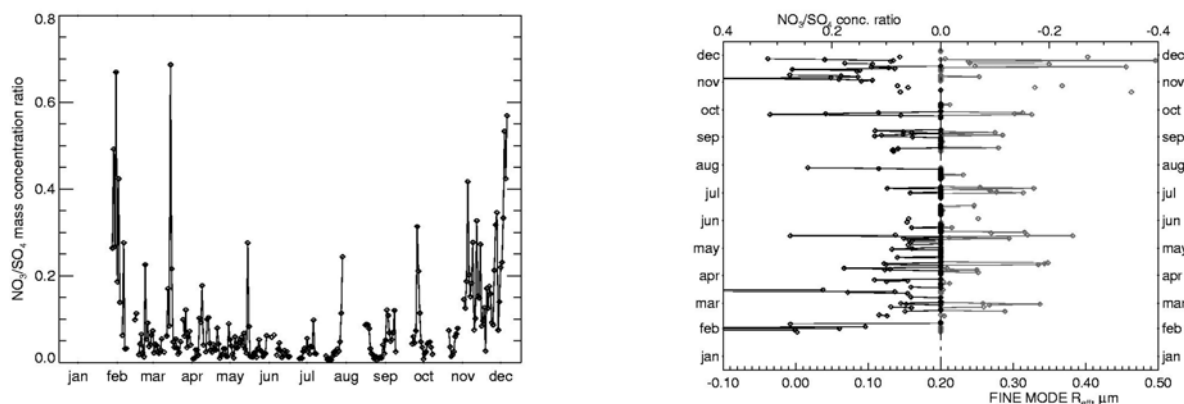


**Figure 3.** Left: ratios of  $\text{NO}_3/\text{SO}_4$  ion mass concentrations in submicron particulate matter measured in the year 2000 at SGP Central Facility by NOAA Pacific Marine Environmental Lab (PMEL). Right: Comparison between these ratios (left) and the fine mode effective radius time series (right) for E13 site from Figure 1 (left bottom panel). The ratios less than 0.05 are set to zero to reflect the lower limit of 0.2  $\mu\text{m}$  in our retrievals of  $r_{\text{eff}}$

## Comparison with AERONET Almucantar Scan Retrievals

We compared our results with the total, fine, and coarse AOTs obtained from AERONET almucantar retrievals (Dubovik and King 2000) for 870, 670, and 440 nm CIMEL sunphotometer channels (the 440 nm results were compared with optical thickness interpolated from MFRSR 415 and 500 nm channels with no  $\text{NO}_2$  subtracted). We used the data from the CIMEL sunphotometer collocated with the two SGP Central Facility MFRSRs (C1 and E13). While showing good agreement on average in total AOT (Figure 4) and Angstrom exponents, our retrievals have a small positive bias of 0.01 (or 10%) on average for fine mode AOT compared with the AERONET values (and a corresponding negative bias for coarse mode AOT). This bias appeared to be caused by the difference in  $\text{NO}_2$  treatment in the two algorithms. Neglect of  $\text{NO}_2$  absorption in AERONET approach effectively causes misinterpretation of this absorption as a contribution from very small aerosol particles. This decreases the retrieved size of fine mode aerosol and increases the coarse mode fraction in AOT, so that the Angstrom exponent in the longwave spectral region outside  $\text{NO}_2$  absorption band remains intact. This relative increase of the coarse mode fraction in AOT and the corresponding increase in the fine mode fraction in AERONET retrievals compared to our values are well seen in Figure 4. The fine mode effective radius in AERONET retrievals for the period of the comparison were always lower than our effective retrieval limit of 0.2  $\mu\text{m}$ , thus they are not suitable for a quantitative comparison. Domination of small ( $\leq 0.2 \mu\text{m}$ ) particles at the SGP Central Facility is in qualitative agreement with our results for the year 2000, however we also detect a number of days when the aerosols were notably larger. However, our retrievals made under zero  $\text{NO}_2$  assumption (grey curves in Figure 1), same as used in AERONET algorithm, show good agreement in fine mode  $r_{\text{eff}}$  with AERONET values (Figure 5). They are only by about 0.015  $\mu\text{m}$  on average, and showing 55% correlation). This confirms that our differences with AERONET in aerosol size retrievals are primarily due to differences of approaches to  $\text{NO}_2$  absorption.

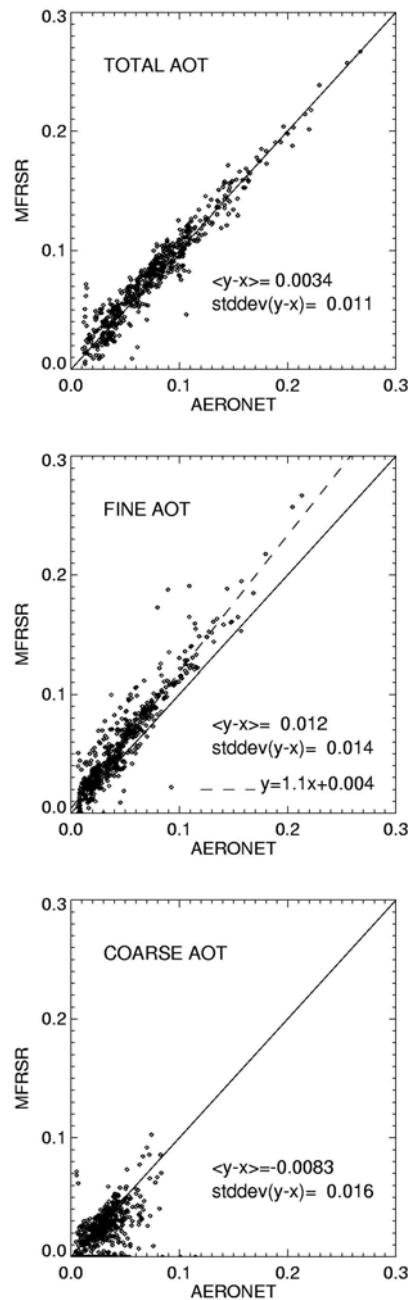


**Figure 4.** Comparison between MFRSR-derived AOTs at 870-nm wavelength (total, fine, and coarse) and those from AERONET almucantar scan analysis. The MFRSR (C1) and CIMEL sunphotometers are located at the SGP's Central Facility. The measurements from March 1998 to September 2000 were used (576 datapoints). The plots show that the presented mode separation method produces slightly higher values of fine mode AOT (and, correspondingly, lower values of coarse AOT) than the AERONET retrievals. The difference in fine AOT can be characterized either as 0.01 on average or as 10% of the AERONET values (the latter is shown by the dashed line).

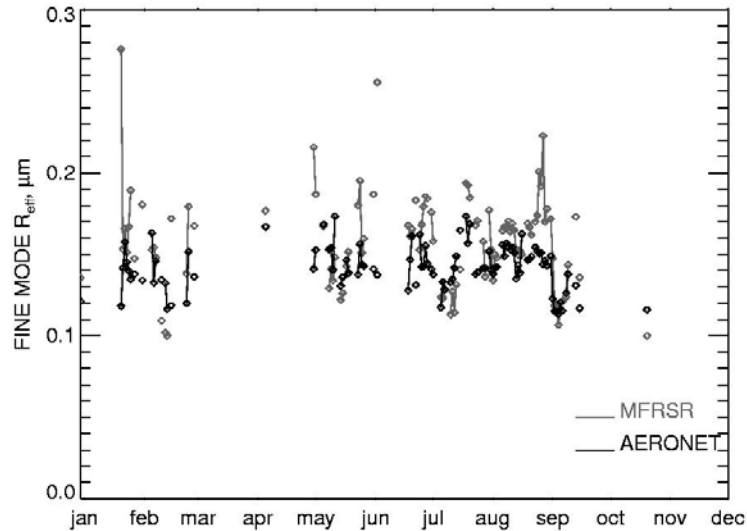


**Figure 5.** Time series of daily mean fine mode effective radii retrieved from AERONET almucantar measurements and from MFRSR data for the same days. MFRSR values are obtained under zero NO<sub>2</sub> constraint.

## Contact

M. Alexandrov, [malexandrov@giss.nasa.gov](mailto:malexandrov@giss.nasa.gov), (212) 678-5548

## References

Alexandrov, MD, BE Carlson, AA Lacis, and B Cairns. 2005. "Separation of fine and coarse aerosol modes in MFRSR datasets." *Journal of Geophysical Research* (Accepted)

Dubovik, O, and MD King. 2000. "A flexible inversion algorithm for retrieval of aerosol optical properties from Sun and sky radiance measurements." *Journal of Geophysical Research* 105, 20,673-20,696.